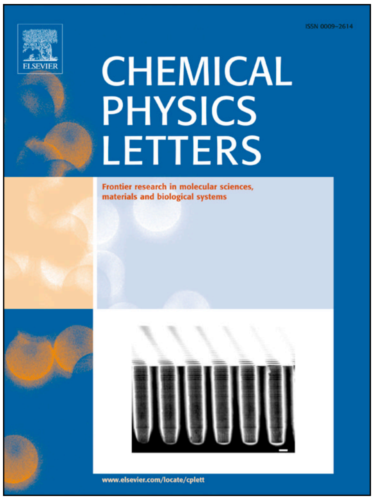

Research paper

Synthesis, Characterization and Relativistic DFT Studies of *fac*-Re$(CO)_3$(isonicotinic acid)$_2$Cl complex

César Zúñiga, Diego P. Oyarzún, Rudy Martin-Transaco, Mauricio Yáñez-S, Alejandra Tello, Mauricio Fuentealba, Plinio Cantero-López, Ramiro Arratia-Perez

PII: S0009-2614(17)30912-0
DOI: https://doi.org/10.1016/j.cplett.2017.09.065
Reference: CPLETT 35145

To appear in: *Chemical Physics Letters*

Received Date: 30 August 2017
Accepted Date: 28 September 2017

Please cite this article as: C. Zúñiga, D.P. Oyarzún, R. Martin-Transaco, M. Yáñez-S, A. Tello, M. Fuentealba, P. Cantero-López, R. Arratia-Perez, Synthesis, Characterization and Relativistic DFT Studies of *fac*-Re$(CO)_3$(isonicotinic acid)$_2$Cl complex, *Chemical Physics Letters* (2017), doi: https://doi.org/10.1016/j.cplett.2017.09.065

Synthesis, Characterization and Relativistic DFT Studies of *fac*-$Re(CO)_3$(isonicotinic acid)$_2$Cl complex.

César Zúñiga[1]*, Diego P. Oyarzún[1], Rudy Martin-Transaco[1], Mauricio Yáñez-S[4], Alejandra Tello[5], Mauricio Fuentealba[2], Plinio Cantero-López*[1,3], Ramiro Arratia-Perez[1,3]

[1]Center of Applied Nanoscience (CANS), Facultad de Ciencias Exactas, Universidad Andres Bello, Av. República 275, Santiago, Chile.

[2]Instituto de Química, Pontificia Universidad Católica de Valparaíso, Av. Universidad 330, Curauma, Valparaíso, Chile.

[3]Relativistic Molecular Physics (ReMoPh) Group, Ph.D. Program in Molecular Physical Chemistry, Universidad Andrés Bello, Av. República 275, Santiago, Chile.

[4]Departamento de Ciencias del Ambiente, Facultad de Química y Biología, Universidad de Santiago de Chile, Santiago, Chile.

[5]Laboratorio de nanotecnología, recursos naturales y sistemas complejos, Facultad de Ciencias Naturales, departamento de Química y Biología, Universidad de Atacama, Copayapu 485, Copiapó, Chile.

Keywords: Rhenium (I) complex, isonicotinic acid, relativistic DFT calculations, UV–vis spectrum.

Abstract

In this work, new *fac*-$Re(CO)_3(PyCOOH)_2Cl$ from isonicotinic acid ligand has been prepared. The complex was characterized by structural (single-crystal X-ray diffraction), elemental analysis and spectroscopic (FTIR, NMR, UV-vis spectroscopy) methods. DFT and TDDFT calculations were performed to obtain the electronic transitions involved in their UV–Vis spectrum. The excitation energies agree with the experimental results. The TDDFT calculations suggest that experimental mixed absorption bands at 270 and 314 nm could be assigned to (MLCT-LLCT)/MLCT transitions. Natural Bond Orbitals (NBO) approach has enabled studying the effects of bonding interactions. E(2) energies confirm the occurrence of ICT (Intra-molecular Charge Transfer) within the molecule.

1. Introduction

In the last decades, the preparation of new transition-metal complexes with pyridine derivate ligands have attracted increasing interest due to their application in several fields of chemistry [1-3]. In this context, Re(I) compounds containing the *fac*-$[Re(CO)_3]^+$ moiety are considered prospective materials due to their potential applications in a wide range of applications, such as microscopy, organic light-emitting diode (OLED) [4], photosensitizers in solar cells [5], sensors and biomedical purposes, due to their unique photophysical and photochemical properties [6-7]. In this sense, the photochemical properties have been studied for electrocatalytic and photocatalytic reduction of CO_2 to CO [8-11].

The most recent and significant applications of these compounds are their use as therapeutic and radiopharmaceutical agents. For instance, *fac*-tricarbonylrhenium(I) complexes serve as cold analogs for radioactive ^{99m}Tc(I) biological imaging agents.[12-15]. All these interesting properties increase the interest of the scientific community in the synthesis and study of this type of compounds. Consequently, ligands that can act as good coordination agents are needed. For this purpose, nicotinic derivatives, e.g. such as isonicotinic acid have been widely used as monodentate and bridging ligands through their pyridine and/or carboxylate end [16-17].

Re(I) complexes are normally synthetized from the $Re(CO)_5X$ (X = Cl or Br) as starting material, the strong *trans* directing influence of the CO ligands results in the facile substitution of two equivalents of CO that are *cis* to one another. Carbon monoxide is a classic ligand in inorganic chemistry for describing back-bonding concept. In organometallic chemistry, back-bonding described as a donation of electron density from a filled nonbonding d-orbital, with an appropriate symmetry, to the LUMO in a carbon monoxide ligand, producing a new anti-bonding of orbital character (π*) . The result of this interaction is a stronger metal-carbonyl bond [17].

From a theoretical point of view, compounds of heavy metals and their properties are influenced by relativistic effects [18-19]. This can be observed in the energy stabilization of occupied and virtual orbitals. For instance, usually in the case of scalar-relativistic calculations produce a destabilization as a product of the indirect relativistic effects over d in comparison to non-relativistic calculations, but these orbitals are re-stabilized by the spin-orbit coupling effect. This in turn has an influence on the correct determination of the spectroscopic properties, among others. In this context, during the last decade, there has been much interest in the study of electronic structure and spectroscopic properties of Rhenium complexes, using relativistic density functional theory (RDFT) [20]. New progress on this matter provides a convenient opportunity for the theoretical study of absorption energies of in organic and inorganic molecules through of Relativistic Time- Dependent Density Functional Theory (TD-RDFT). This methodology provides important information about the nature of the electronic transitions involved in the absorption properties of these complexes. [21-22].

On the other hand, intra- and intermolecular bonding properties play an important role in the electronic structure, which have a direct influence on the stability of the molecule, among others relevant properties of Rhenium complexes. In this context, Natural Bond Orbitals (NBO) analysis provides the most probable ‘natural Lewis structure’ picture because all orbital details are mathematically chosen to include the highest possible percentage of the electron density. A useful aspect of the NBO method is the information given about the energy transfer between both filled and virtual orbitals, which could improve the analysis of intra- and inter-molecular interactions [23].

In the present work, we report the synthesis and characterization by IR, NMR, UV–vis spectroscopy, single crystal X-ray analysis and elemental analysis of the new tricarbonyl rhenium (I) complex with isonicotinic acid (PyCOOH) as ligand, *fac*-$Re(CO)_3(PyCOOH)_2Cl$. TDDFT studies were used to identify the main electronic transitions whereas NBO analysis enabled the study of the intra-molecular charge transfer properties.

2. Experimental Section

2.1. General Procedure

The reaction was performed under an atmosphere of argon. The organic solvents were dried before use, using the appropriate drying reagents. $Re(CO)_5Cl$ and Isonocotinic acid (PyCOOH) were purchased from Aldrich, and used as received. Infrared spectra were recorded on a Perkin-Elmer FTIR Spectrum Two coupled to a UATR unit. The sample was directly positioned over the diamond, pressed up to 30% of the total supported pressure and scanned in the range of 4000 to 500 cm^{-1} with a resolution of 1 cm^{-1}.^1H NMR and $^1H–^1H$ COSY spectra were recorded on a Bruker AVANCE 400 spectrometer, all spectra being referred to TMS as an internal standard. Electronic spectrum was measured on a spectrophotometer Perkin-Elmer Lamda 35 with resolution of 1 nm using 1 cm quartz cells in the range 800-200 nm. Elemental analyses were performed using a EA 1108 CE Instruments elemental analyzer.

2.2. Synthesis of *fac*-$Re(CO)_3(PyCOOH)_2Cl$

Rhenium pentacarbonyl chloride (100 mg, 0.28 mmol) and isonicotinic acid (123 mg, 0.56 mmol) were dissolved in 1:1 tetrahydrofuran:toluene (40 mL) and heated to reflux for 2 days. The reaction mixture was cooled at room temperature and the solvent was removed by rotary evaporation, the solid was then redissolved in 1:1 THF:toluene (6mL), and precipitated with petroleum ether. The solid was filtered and washed with small portions of petroleum ether and dried under vacuum. Yield: 115 mg, 74%. Anal. Calc. for $ReC_{15}H_{10}N_2O_7Cl{\bullet}H_2O$: C, 31.61; H, 2.12; N, 4.92. Found: C, 32.01; H, 2.14; N, 4.93% IR, ATR (cm^{-1})νC–O = 2024, 1882 and–COOH 1717.^{1}H NMR ($(CD_3)_2CO$) δ (ppm), *J*(Hz): 9.07 (d, 4H, Ha, *J* = 5.62); 8.06 (d, 4H, Hb, *J* = 5.87). ^{13}C NMR ($(CD_3)_2CO$) δ (ppm): 205.25; 164.22; 154.88; 140.19; 125.28.

X-ray quality crystals of complex $Re(CO)_3(PyCOOH)_2Cl$ were grown by vapor diffusion of petroleum ether into a solution of the complex, previously dissolved in acetone.

2.3. X-ray Crystal Structure Determination for *fac*-$Re(CO)_3(PyCOOH)_2Cl$.

X-ray suitable crystals were obtained as described above. A suitable single crystal was mounted using a MiTeGen MicroMounts. Table 1 shows experimental and crystallographic data for the obtained complex. On the other hand, selected bond distances and angles are reported in Table 2, and intermolecular interactions are summarized in Table 3. Intensity data was collected at room temperature on a Bruker D8 QUEST diffractometer equipped with a bidimensional CMOS Photon100 detector, using graphite monochromated Mo-Kα radiation. The diffraction frames were integrated by means of the APEX2 package and were corrected for absorptions with SADABS. The solution and refinement for the Re(I) complex was carried out with Olex2 [24]. The structure was solved with Direct Methods using the ShelXS software [25]. The complete structures were refined by the full matrix least-squares procedures on the reflection intensities (F^2) with the ShelXL [24]. All non-hydrogens were refined with anisotropic displacement coefficients, and all hydrogen atoms were placed in idealized locations.

3. Results and Discussion

3.1. Synthesis and Characterization

The new Re(I) complex was prepared by mixing one equivalent of [$Re(CO)_5Cl$] compound and two equivalents of the isonicotinic acid in refluxing tetrahydrofuran: toluene(1:1, v/v) for 24 hours, as shown in Scheme 1. Pyridine derivatives generally require longer reflux time to fully react [26]. The obtained complex is stable in air, microcrystalline solid, and soluble in common organic solvents.

The metal center has an almost ideal octahedral coordination sphere with a facial arrangement of three carbonyl groups. The typical *fac*-tricarbonyl unit in this complex is evidenced by the CO stretching frequencies in the IR spectrum of the complex and confirmed by the X-ray crystal structure.

The IR spectrum of the complex showed two bands in the carbonyl stretching region, one sharp and the other broad, at 2014 cm^{-1} and 1882 cm^{-1}, respectively. The broader band has been assigned as a combination of the carbonyl ligands "*trans*" to the pyridines [27]. The typical stretching band of carbonyl, from carboxylic acid, was recorded at 1717 cm^{-1} due to vibration of the C=O acid group.

The coordination of the isonicotinic acid to the Re(I) elicits a downfield shift of the proton peaks of the isonicotic acid with respect to the free ligand. The ^{1}H-NMR and

^{13}C-NMR spectra were in agreement with the proposed structure of the complex, the proton NMR spectrum has two doublet resonances at 9.07 (Ha) and 8.06 (Hb), which may be attributed to the pyridine protons. The IR and NMR spectra are included as supplementary material.

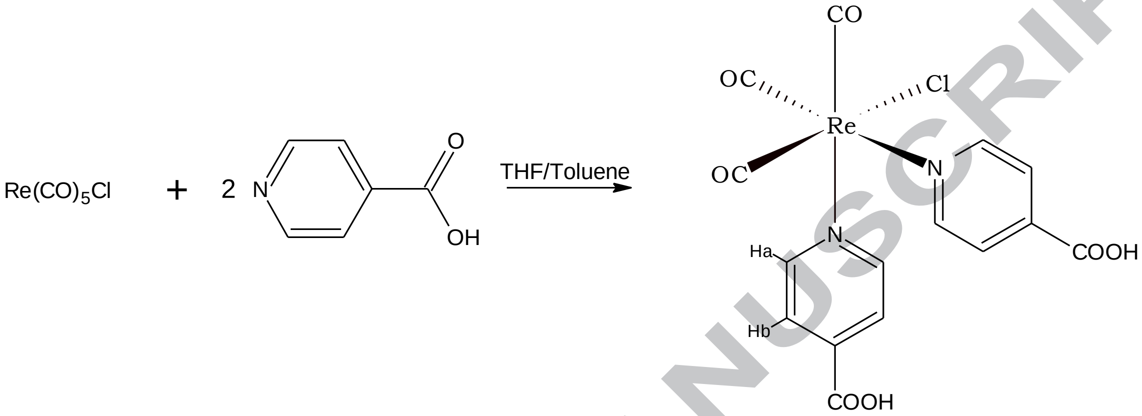

Scheme 1. Synthesis of complex.

3.2. Crystal Structure

ORTEP drawing of *fac*-Re(CO)$_3$(PyCOOH)$_2$Cl compound along with the full atom numbering scheme are shown in Figure 1. The title compound crystallizes in the monoclinic P2$_1$/n space group showing, in the asymmetric unit, the rhenium complex and one water solvate molecule. The rhenium center displays an octahedral geometry with two isonicotinic acid ligands in *cis* conformation, three carbonyl ligands in *fac* conformation and, one chlorine ligand *trans* to one carbonyl ligand. The octahedral geometry can be confirmed for the following features: (i) the sum of the absolute value of the deviation of all 12 *cis* angles from 90° is 32.5(12)º, (ii) the angles between the *trans* ligands are close to 180º and, (iii) the deviation of the rhenium center from the octahedron centroid is 0.150(2) Å.

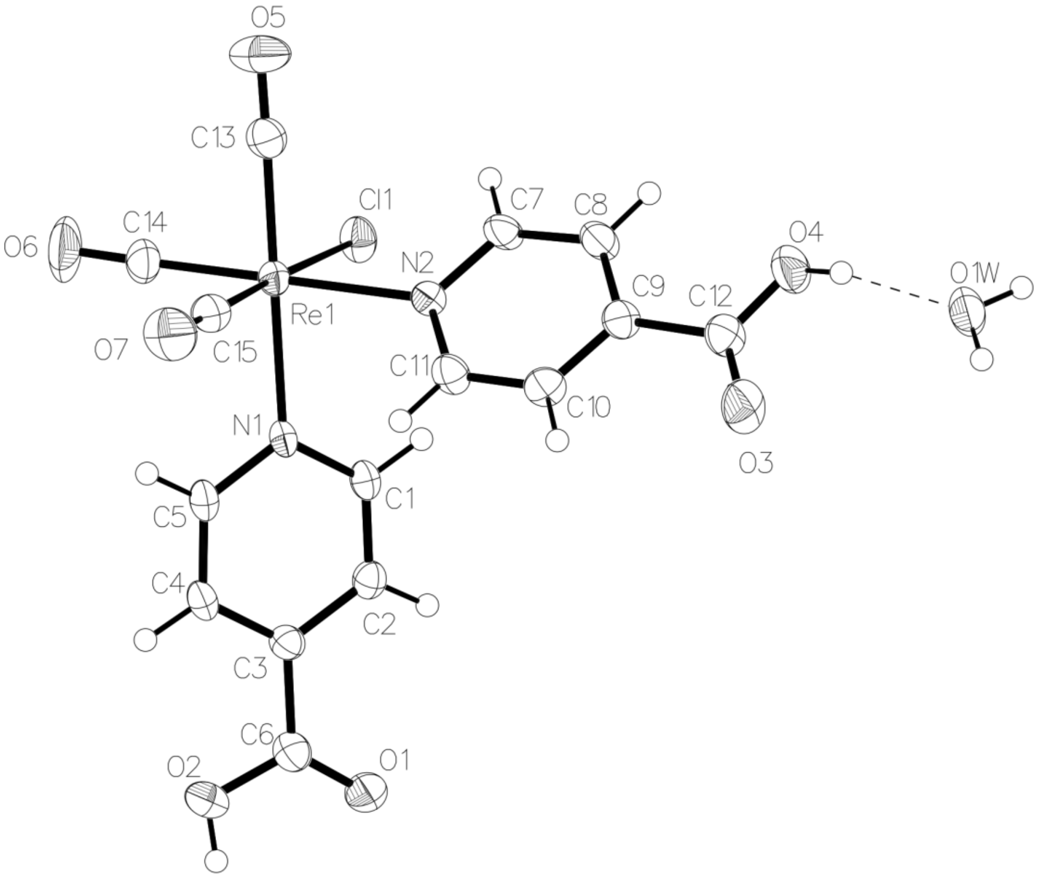

Figure 1. Molecular structure of ***fac*-Re(CO)$_3$(PyCOOH)$_2$Cl·H$_2$O** with the atom numbering scheme. Thermal ellipsoids are drawn at 30% probability.

As expected, the bond lengths between the metal center and the ligands are different with (mean) values of 1.907 for carbonyl ligands, 2.212 for isonicotinic acid ligands and, 2.469 for chlorine ligand.

The dihedral angles between the least-square planes [C13-C15-Cl1-N1] and [C14-C15-Cl1-N2] with the phenyl rings of his corresponding isonicotinic acid ligands are 41.80(19) and 42.18(19)º, respectively.

One intermolecular hydrogen bond is observed for two complexes between the carboxylic acid functional groups, O2-H2A···O3 (-1/2+x, 5/2-y, -1/2+z). Additionally, two intermolecular hydrogen bonds are formed between the complexes and the water molecule, O4-H4···O1W and O1W-H1WB···O1 (1/2+x, 5/2-y,1/2+z). This set of intermolecular interactions builds a tenth-membered ring. The crystal structure is stabilized by this network of intermolecular hydrogen bonds generating infinite zig-zag chains in the [1 0 1] direction (see Figure 2).

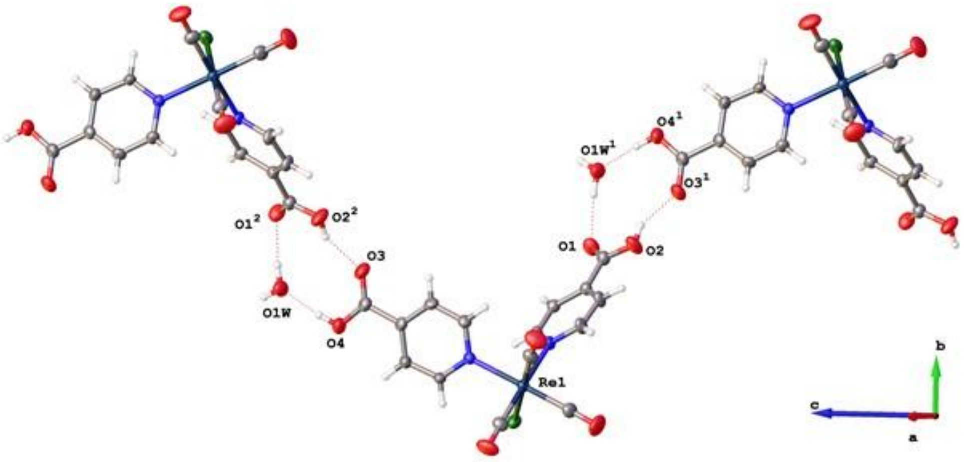

Figure 2. Intermolecular hydrogen bond interactions. Symmetry codes: ^{1} (-1/2+x, 5/2-y, -1/2+z); ^{2} (1/2+x, 5/2-y,1/2+z).

Table 1. Crystal data collection and structure refinement parameters for ***fac*-Re(CO)$_3$(PyCOOH)$_2$Cl**.

Empirical formula	$C_{15}H_{12}ClN_2O_8Re$
Formula weight	569.92
Temperature/K	296.15
Crystal system	monoclinic
Space group	$P2_1/n$
a/Å	13.8283(6)
b/Å	6.9775(3)
c/Å	20.0599(8)
α/°	90
β/°	95.568(2)
γ/°	90
Volume/Å^3	1926.39(14)
Z	4
ρ_{calc}g/cm^3	1.965
μ/mm^{-1}	6.490
F(000)	1088.0
Crystal size/mm^3	0.343 × 0.154 × 0.103
Radiation	MoKα (λ = 0.71073)
2Θ range for data collection/°	5.92 to 53.374
Index ranges	$-17 \le h \le 17$, $-8 \le k \le 8$, $-25 \le l \le 25$
Reflections collected	52396
Independent reflections	4068 [R_{int} = 0.0486, R_{sigma} = 0.0182]

Data/restraints/parameters	4068/0/248
Goodness-of-fit on F^2	1.284
Final R indexes [I>=2σ (I)]	R_1 = 0.0345, wR_2 = 0.0658
Final R indexes [all data]	R_1 = 0.0444, wR_2 = 0.0690

Table 2 Selected bond distances (Å) and angles (°) for ***fac*-Re(CO)$_3$(PyCOOH)$_2$Cl**.

Bond distances (Å)	
Re1-Cl1	2.4694(16)
Re1-N1	2.212(5)
Re1-N2	2.212(5)
Re1-C13	1.914(7)
Re1-C14	1.905(7)
Re1-C15	1.903(8)
Angles (°)	
N1-Re1-Cl1	85.80(13)
N1-Re1-N2	86.44(17)
N2-Re1-Cl1	86.06(13)
C13-Re1-N1	178.1(2)
C13-Re1-Cl1	92.4(2)
C13-Re1-N2	94.1(2)
C14-Re1-N1	92.7(3)
C14-Re1-Cl1	91.6(2)
C14-Re1-N2	177.6(3)
C14-Re1-C13	86.7(3)
C15-Re1-N1	92.2(2)
C15-Re1-Cl1	177.9(2)
C15-Re1-N2	93.2(3)
C15-Re1-C14	89.1(3)
C15-Re1-C13	89.6(3)

Table3. Hydrogen Bonds for ***fac*-Re(CO)$_3$(PyCOOH)$_2$Cl**.

D-H···A	D-H (Å)	H···A (Å)	D···A (Å)	∠D-H···A (°)
O2-H2A···O3^1	0.82	1.92	2.672(7)	151.4
O4-H4···O1W	0.82	1.79	2.560(7)	155.0
O1W-H1WB···O1^2	0.85	1.96	2.798(8)	168.0

Symmetry codes: ^{1} (-1/2+x, 5/2-y, -1/2+z); ^{2} (1/2+x, 5/2-y,1/2+z)

3.3. UV–Vis Absorption Spectra

The electronic spectrum of the *fac*-$Re(CO)_3(PyCOOH)_2Cl$ complex and PyCOOH ligand, both recorded in CH_3CN, are shown in Figure 3. The band at 279 nm ($1.1 \bullet 10^4$ M^{-1} cm^{-1}) was assigned to the $\pi \rightarrow \pi*$ transitions in the PyCOOH ligand coordinated to Re(I). As a reference, in the UV-Vis spectrum of the ligand, this band is recorded at 270 nm. In the complex, this band appeared red shifted, probably due to the coordination of PyCOOH ligand to the Re(I). The band observed at 314 nm ($9.6 \bullet 10^3$ M^{-1} cm^{-1}) with a tail lying into the visible region, is assigned to the Re(I)$\rightarrow$PyCOOH charge transfer with a certain contributions of the $\pi \rightarrow \pi*$ intraligand transitions mentioned before [28].

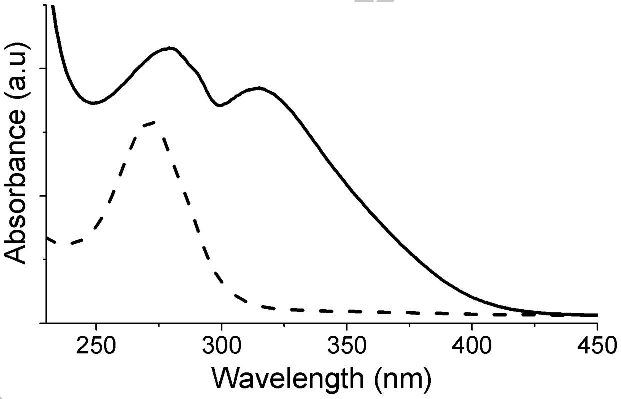

Figure 3. UV-Vis spectrum of *fac*-$Re(CO)_3(PyCOOH)_2Cl$ (solid line) and PyCOOH (dashed line)

3.4. Quantum Chemistry Calculations

All the calculations for the complex reported here were carried out in the framework of the relativistic density functional theory (RDFT) using the Amsterdam Density Functional computational package (ADF code) via the zeroth-order regular approximation (ZORA) Hamiltonian including the relativistic corrections. [29]

3.4.1 Geometry

The geometries were optimized at BP86/TZ2P level of theory. The most important geometrical parameters are listed in Table 4. The bond lengths around the Rhenium(I) metal center and CO ligand are consistent with the experimental X-ray single crystal data. Frequency calculations were performed on Rhenium (I) complex. All their values were real, confirming that the structures are minimal on the potential energy surface. On the other hand, good correlation between theoretical values of the CO frequency and available experimental results was observed. The calculated frequencies are consistent with the fact that the back-donation to π* empty molecular orbitals in CO ligand (free ν_{CO} = 2143 cm^{-1}) [30].

Table 4. Optimized geometries for *fac*-$Re(CO)_3(PyCOOH)_2Cl$ at BP86. All distances are in angstrom (Å) and frequencies in cm^{-1}

Molecule	**Experimental**	**Calculated**
***fac*-$Re(CO)_3(PyCOOH)_2Cl$**		
d(Re-Cl)	2.47	2.51
d(Re-CO)	1.92	1.92
d(Re-(PyCOOH))	2.21	2.23
d(CO)	1.14	1.17
ν(sym)	1830	
ν(asym)	1858	

3.4.2 TD-DFT Calculations

To calculate optical properties Scalar Relativistic Time Dependent Density Functional Theory (SR-TDDFT) was employed to find the energies for the first 100 excitations. The calculations were performed in acetonitrile and gas phase by using the standard BP86/TZ2P level of theory. Environmental effects were included via COSMO continuum solvation using acetonitrile parameters. The most important transition appears in the region between 247 and 327 nm (see Figure 4), which is in good agreement with the experimental values. The energy (in eV) and the composition in terms of contributions from the different groups to the MO of the main lowest virtual MOs and highest occupied MOs involved in the computed excitations are shown in Table 5. The HOMO orbital of the *fac*-Re(CO)$_3$(PyCOOH)$_2$Cl is mainly composed of a bonding combination d orbitals of the Re atom (51.8%), a chloride orbital (33%) and π orbital of the CO ligands. The composition of LUMO orbital includes only π orbital of the ancillary ligand (100%).

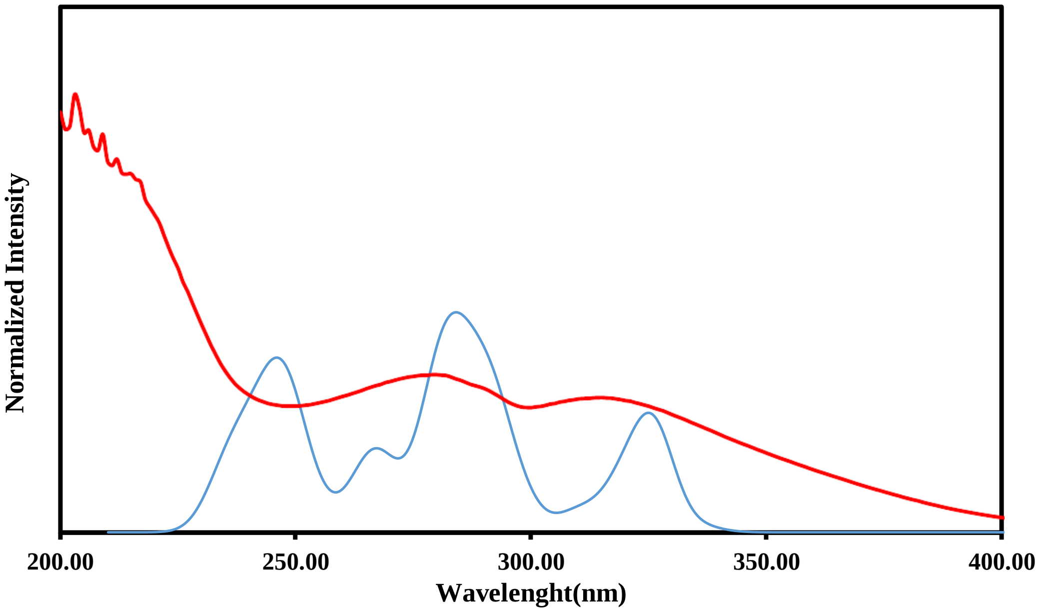

Figure 4. Experimental (red line) vs computed (blue line) electronic absorption spectra of *fac*-Re(CO)$_3$(PyCOOH)$_2$Cl (solvent included) (BP86/TZ2P). The spectra was simulated using Lorentzian curves.

Table 5. Energies and composition (%) of the MOs of the *fac*-Re(CO)$_3$(PyCOOH)$_2$Cl. All values were obtained via COSMO continuum solvation using acetonitrile parameters.

MO	ev	Contributions (%)			
		Re	CO	Cl	(PyCOOH)ligand
LUMO+1	-7.56	0	0	0	100
LUMO	-7.57	0	0	0	100
HOMO	-10.03	52	15	33	0
HOMO-2	-10.35	67	30	0	3
HOMO-3	-11.23	7	0	19	73
HOMO-4	-11.27	49	1	16	34
HOMO-6	-11.47	3	0	26	71
HOMO-12	-12.22	7	6	2	86

Table 6 and Figure 5 list the most important lower singlet excited states along with the corresponding wavelength of the transition from the ground state, the calculated oscillator strength and the major contributions to the final wavefunction.

Table 6. Maximum absorption wavelengths (nm), molar extinction coefficients (L $mol^{-1}cm^{-1}$) (determined experimentally), and maximum absorption wavelengths (nm), and nature of the electronic transitions (determined by TD-DFT calculations) for *fac*-$Re(CO)_3(PyCOOH)_2Cl$.

	λ_{exp}	ε	λ_{calc}	f	Assignment
	314	9578	327	3.01E-02	MLCT(HOMO-4→LUMO+1)(88%)
Acetonitrile	270	11465	280	6.80E-02	LLCT(HOMO-6→LUMO)(97%)
			268	5.91E-02	MLCT(HOMO-2→LUMO)(83%)
			247	4.02E-02	LLCT(HOMO-12→LUMO)(97%)
Gas			355	4.06E-03	MLCT(HOMO→LUMO+4)(95%)
			315	2.00E-05	LLCT(HOMO→LUMO+5)(93%)
			278	4.32E-03	MLLCT(HOMO-2→LUMO)(84%)
			257	2.97E-04	LLCT(HOMO-3→LUMO+3)(96%)

According to the calculated transitions, the band centered at 314 nm in the experimental spectrum may originate by electronic transitions from HOMO-4→LUMO+1 and can be assigned as a MLCT. The second band centered at 270 nm was assigned as LLCT(HOMO-6→LUMO) transitions and obey to $\pi-\pi^*$ excitations into isonicotinic acid ligand. This band has also some contribution from the MLCT (HOMO-2→LUMO) state, which was mainly assigned to d-π^* (Re→(PyCOOH)). The third band centered at 247 nm can be assigned as LLCT(HOMO-12→LUMO) and is characterized by $\pi-\pi^*$ transitions in (PyCOOH) ligand with some contributions of charge transfer from CO ligands, Re(I) atom to the ancillary ligand.

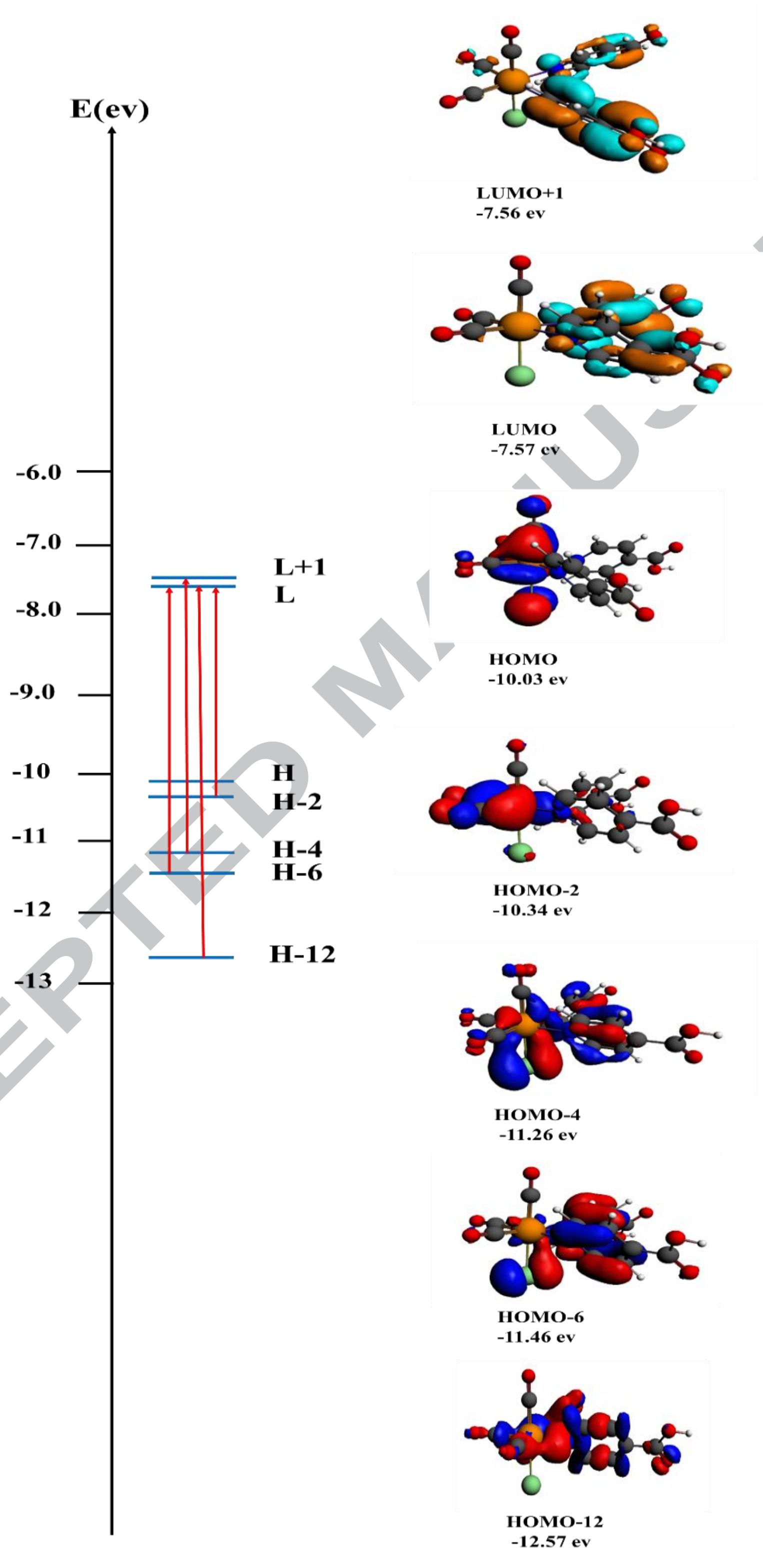
E(ev)
-6.0
-7.0
-8.0
-9.0
-10
-11
-12
-13
L+1
L
H
H-2
H-4
H-6
H-12
LUMO+1
-7.56 ev
LUMO
-7.57 ev
HOMO
-10.03 ev
HOMO-2
-10.34 ev
HOMO-4
-11.26 ev
HOMO-6
-11.46 ev
HOMO-12
-12.57 ev

Figure 5. Qualitatively Molecular Orbital diagram for fac-Re(CO)$_3$(PyCOOH)$_2$Cl with the most important electronic transitions. Gradient isosurface (0.03 a.u.).

3.4.3 NBO Analysis

To get a more comprehensive picture about of the interactions in *fac*-Re(CO)$_3$(PyCOOH)$_2$Cl, Natural Bond Orbital analysis (NBO) was performed. This method provides an efficient way to study intra- and intermolecular bonding and interaction between molecular fragments. Additionally, NBO gives a convenient basis set to investigate charge transfer in molecular systems [31-33]. The second-order Fock matrix was carried out to evaluate the donor and acceptor interactions in the NBO analysis, for each donor (i) and acceptor (j), the stabilization energy E(2) associated with the delocalization i→j is estimated as:

$$E(2) = \Delta E_{ij} = q_i \frac{F(i,j)^2}{E_i - E_j}$$

where q_i is the donor orbital occupancy, E_i and E_j are diagonal elements and $F(i,j)$ is the diagonal NBO Fock matrix element. The larger the E(2) value indicate that there is a strong interaction between electron donor and electron acceptor. The scheme used and results obtained are shown in Figure 6 and Table 7 respectively.

Table 7. Second-order perturbation theory analysis of Fock matrix in NBO basis^a

Donor(i)	Type	Acceptor(j)	Type	E(2) (kcalmol $^{-1}$)	E(j)−E(i) b(a.u.)	F(i,j)c(a.u.)
N 1- C4	BD	Re	RY*	41.45	9.91	0.10
N 1- C5	BD	Re	RY*	56.29	6.84	0.12
N 2- C6	BD	Re	RY*	50.98	9.44	0.03
N 2- C7	BD	Re	RY*	48.28	7.22	0.04
Cl	LP	Re-C	BD	128.55	0.49	0.02

C1- O1	BD	Re	RY*	191.93	7.18	0.12
C2-O2	BD	Re	RY*	228.50	5.68	0.16
C3- O3	BD	Re	RY*	184.38	6.05	0.10
Re	RY*	C1- O1	BD	15.03	6.2	0.11
Re	RY*	C2-O2	BD	13.48	6.26	0.03
Re	RY*	C3- O3	BD	12.71	6.17	0.03

a **BD= bonding orbitals, LP= lone pair , RY= Rydberg**

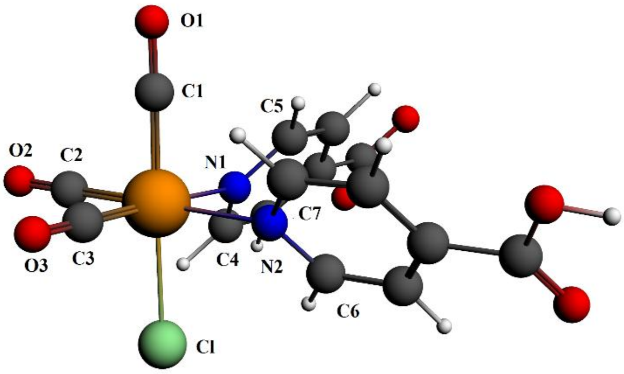

Figure 6. Scheme used in NBO analysis

From Table 7 the NBO analysis clearly evidences the intramolecular charge transfer leading to stabilization of the complex and is related to electron donating from a) bonding of N_1- $C_{(4,5)}$ and N_2- $C_{(6,7)}$ to Rydberg (RY*) in Rhenium(I) atom b) Cl lone pair to bonding of Rhenium (I) atom c) electron-donation from bonding of CO group to RY* in Rhenium(I) atom. Another important interaction is the back –donation from metal orbitals in the metal to the π* empty molecular orbitals in CO ligand, which is consistent with the frequency analysis mentioned before.

4. Conclusion

In the present work, we have reported the synthesis and a rigorous characterization of a new Re(I) tricarbonyl isonicotinic acid complex. The complex was fully characterized by structural (single-crystal X-ray diffraction), elemental analysis and spectroscopic (FTIR, NMR, UV-vis spectroscopy) and DFT methods.

The theoretical results obtained in this work are in agreement with the experimental data reported for the *fac*-$Re(CO)_3(PyCOOH)_2Cl$ (crystallographic and UV-vis absorption spectrum). The spectroscopic transitions involved are mainly ascribed to (MLCT-LLCT)/ MLCT phenomena. The molecule under study in the present work has a remarkable ICT (Intra-molecular Charge Transfer) within the molecule.

Supplementary Materials

Crystallographic data for the structural analysis has been deposited with the Cambridge Crystallographic Data Centre, CCDC Nos. 1565058. This data can be obtained free of charge from The Cambridge Crystallographic Data Centre via www.ccdc.cam.ac.uk/data_request/cif.

Acknowledgements

We are grateful to project PMI-UAB 1301 of Universidad Andres Bello for the financial support for this study, to the Iniciativa Científica Milenio (ICM) RC 120001 del Ministerio de Economía, Fomento y Turismo del Gobierno de Chile. P.C.L. acknowledges CONICYT PCHA/Doctorado Nacional/2013-63130037 for his PhD fellowship and Andres Bello University (internal project DI-712-15/I). R. M.-T. We also thank the support from the grant FONDECYT-3150205 and M. Y.-S. thanks to DICYT-USACH Project 021541YS. A. T. thanks the Universidad de Atacama for project DIUDA 22339.

5. References

[1] J.R. Farrell, C. Becker, D.P. Lavoie, J.L. Shaw, C.J. Ziegler, J.Organomet. Chem. 689 (2004) 1122.

[2] J.R. Farrell, D.P. Lavoie, R.T. Pennell, A. Cetin, J.L. Shaw, C.J. Ziegler, Inorg. Chem. 46 (2007) 6840.

[3] A. Zarkadoulas, E. Koutsouri, C. Kefalidi, C. A. Mitsopoulou, Coord. Chem. Rev.304–305 (2015) 55.

[4] S. Ranjan, S.-Y. Li, K.-C. Hwang, W.-L. Ching, C.-S. Liu, Y.-T.Tao, C.-H. Chien, S.-M. Peng, G.-H. Lee, Inorg. Chem. 42 (2003) 1248.

[5] Y. Chen, W. Liu, J.-S. Jin, B. Liu, Z.-G. Zou, J.-L. Zuo, X.-Z. You, J. Organomet. Chem. 694 (2009) 763.

[6] A. Sarto Polo, M. Kayoko Itokazu, K. Morelli Frin, A. O. de Toledo Patrocínio, N. Y. Murakami Iha, Coord. Chem. Rev. 350 (2016) 1669.

[7] A. Vlĉek Jr., M. Busby, Coord. Chem. Rev. 250 (2006) 1755.

[8] B. Rezaei, M. Mokhtarianpour, A. Asghar Ensafi, H. Hadadzadeh, J. Shakeri, Polyhedron 101 (2015) 160.

[9] K. A. Grice, Coord. Chem. Rev. 336 (2017) 78.

[10] L.M. Kiefer, J.T. King, K.J. Kubarych, Acc. Chem. Res. 48 (2015) 1123.

[11] M. E. Louis, T. G. Fenton, J. Rondeau, T. Jin, G. Li, Comments Inorg. Chem. 36 (2016) 38.

[12] B.R. Franklin, R.S. Herrick, C.J. Ziegler, A. Cetin, N. Barone, L.R. Condon, Inorg. Chem. 47 (2008) 5902.

[13] R. Alberto, J. Organomet. Chem. 692 (2007) 1179.

[14] S.L. Binkley, N.V. Barone, A.C. Underwood, A. Milsted, B.R. Franklin, R.S. Herrick, C.J. Ziegler, J. Inorg. Biochem. 104 (2010) 632.

[15] C. Moura, F. Mendes, L. Gano, I. Santos, A. Paulo, J. Inorg. Biochem. 123 (2013) 34.

[16] G. Yang, H. G. Zhu, B. H. Liang, X. M. Chen,Dalton Trans. 5(2001) 580.

[17] J. R. Farrell, G. J. Kerins, K. L. Niederhoffer, L. A. Crandall, C. Ziegler, J. Organomet. Chem. 813 (2016) 41.

[18] Heß, B. A., Relativistic Effects in Heavy-Element Chemistry. Berichte der Bunsengesellschaft für physikalische Chemie, 1997, 101(1), 1-10.

[19] P. Cantero-López, D. Páez-Hernández, R. Arratia-Pérez, Chem. Phys. Lett. (2017), doi: http://dx.doi.org/ 10.1016/j.cplett.2017.07.006

[20] A. Carreño, M. Gacitúa, E. Molins, R. Arratia-Pérez, Chem. Pap. (2017) 1-12.

[21] J. Gancheff, P.A. Denis, F.E. Hahn, J. Mol. Struct. (Theochem) 941 (2010) 1.

[22] B. Machura, J. Kusz, D. Tabak, R. Kruszynski, Polyhedron 28 (2009) 493.

[23] S. Sebastian, N. Sundaraganesan,Spectrochim. Acta Mol. Biomol. Spectrosc., 75(3) (2010) 941.

[24] O. V. Dolomanov, L.J. Bourhis, R.J. Gildea, J.A.K. Howard, H. Puschmann, J. Appl. Crystallogr. 42 (2009) 339.

[25] G.M. Sheldrick, A short history of SHELX, Acta Crystallogr. Sect. A Found. Crystallogr. 64 (2007) 112.

[26] L. R. Hill, O. A. Blackburn, M. W. Jones, M. Tropiano, T. J. Sørensen, S. Faulkner, Dalton Trans. 42(2013) 16255.

[27] D. J. Losey, B. A. Frenzel, W. M. Smith, S. E. Hightower, C. G. Hamaker, Inorg. Chem. Commun 30 (2013) 46.

[28] M. R Goncalves, K. P. M. Frin, Polyhedron 97 (2015) 112.

[29] ADF2016, SCM, Theoretical Chemistry, Vrije Universiteit, Amsterdam, The Netherlands.

[30] P. Cantero-López, L. Le Bras, D. Páez-Hernández, R. Arratia-Pérez, Dalton Trans. 44 (2015) 20004.

[31] T. Leyssens, D. Peeters, G. Orpen, J. Harvey, Organometallics 26 (2007) 2637.

[32] T. Joseph, H. Varghese, Y. Panicker, T. Thiemann, K. Viswanathan, C. Alsenoy, T. Manojkumar, Spectrochimica Acta Part A 117 (2014) 413.

[33] E. Kavithaa, N. Sundaraganesana, S. Sebastiana, Spectrochimica Acta Part A 77 (2010) 612.

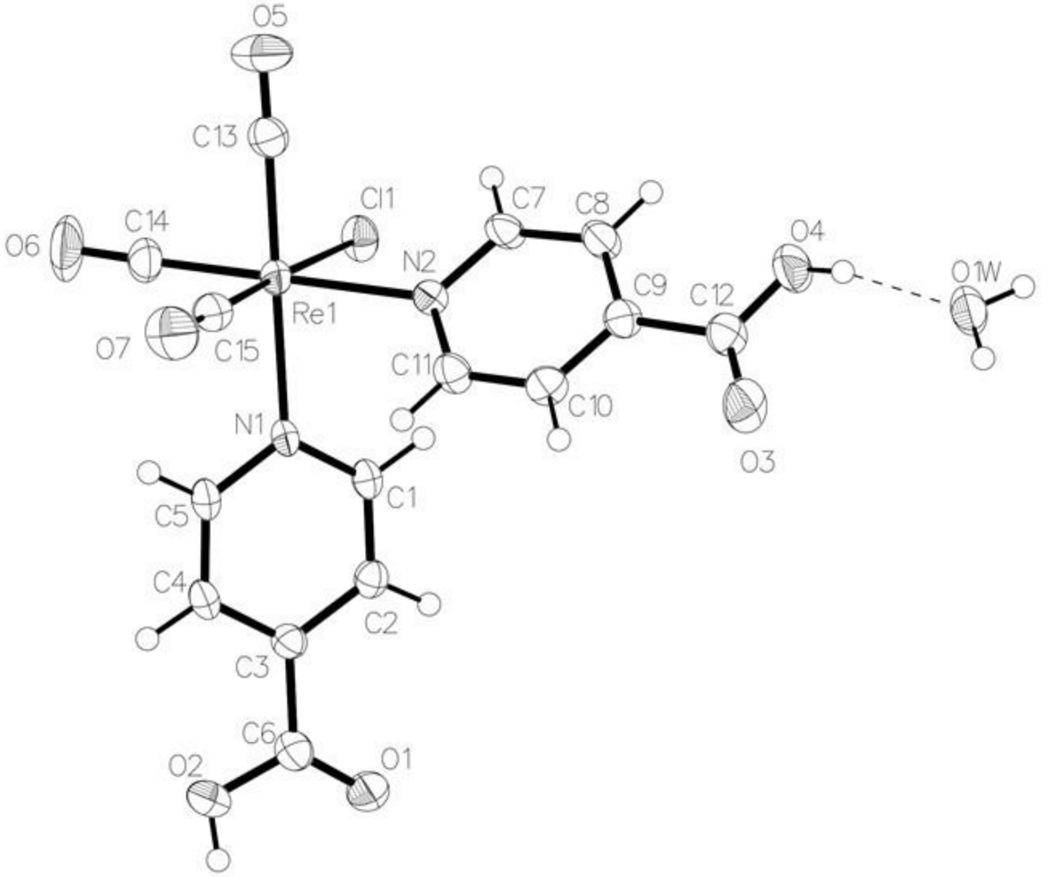

Figure 1. Molecular structure of ***fac*-Re(CO)$_3$(PyCOOH)$_2$Cl·H$_2$O** with the atom numbering scheme. Thermal ellipsoids are drawn at 30% probability.

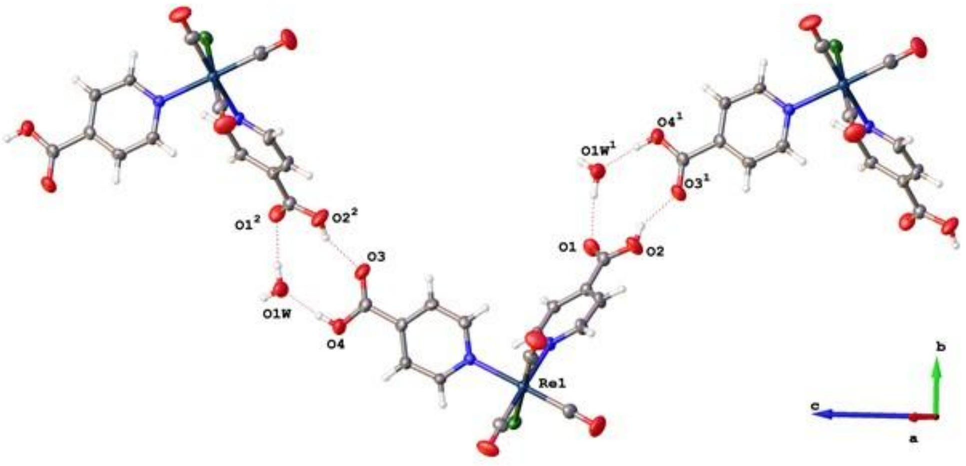

Figure 2. Intermolecular hydrogen bond interactions. Symmetry codes: ^{1} (-1/2+x, 5/2-y, -1/2+z); ^{2} (1/2+x, 5/2-y,1/2+z).

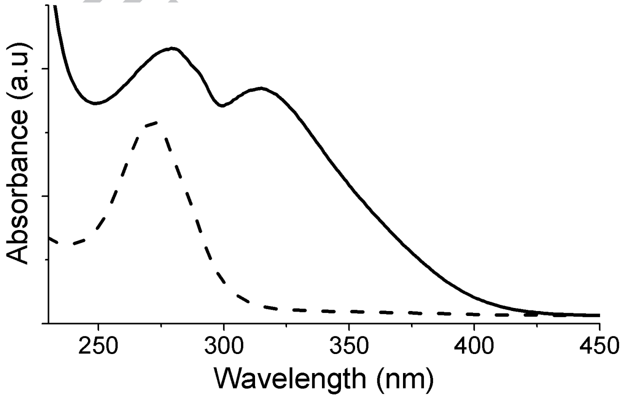

Figure 3. UV-Vis spectrum of *fac*-Re(CO)$_3$(PyCOOH)$_2$Cl (solid line) and PyCOOH (dashed line)

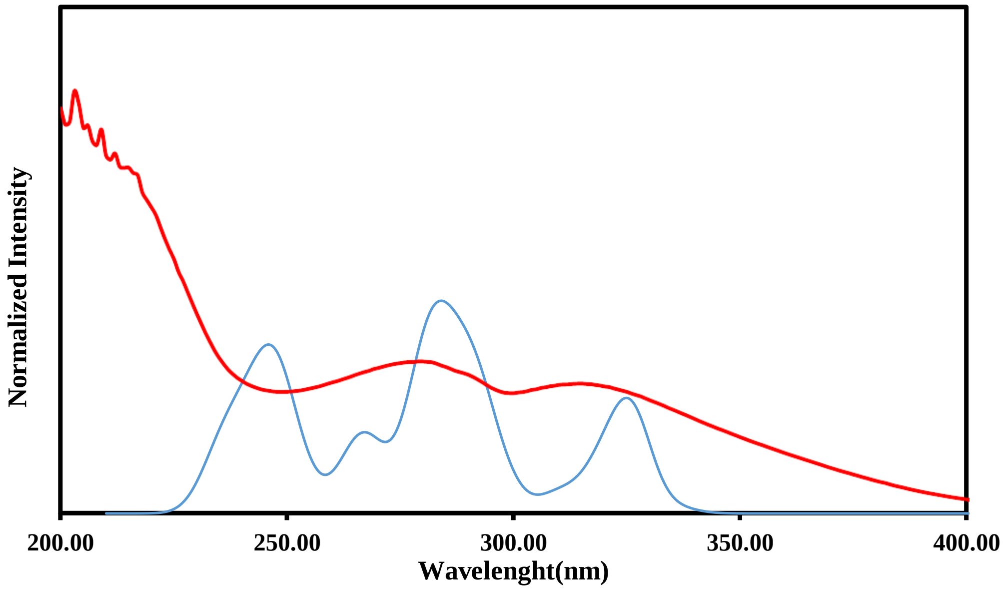

Figure 4. Experimental (red line) vs computed (blue line) electronic absorption spectra of *fac*-Re(CO)$_3$(PyCOOH)$_2$Cl (solvent included) (BP86/TZ2P).

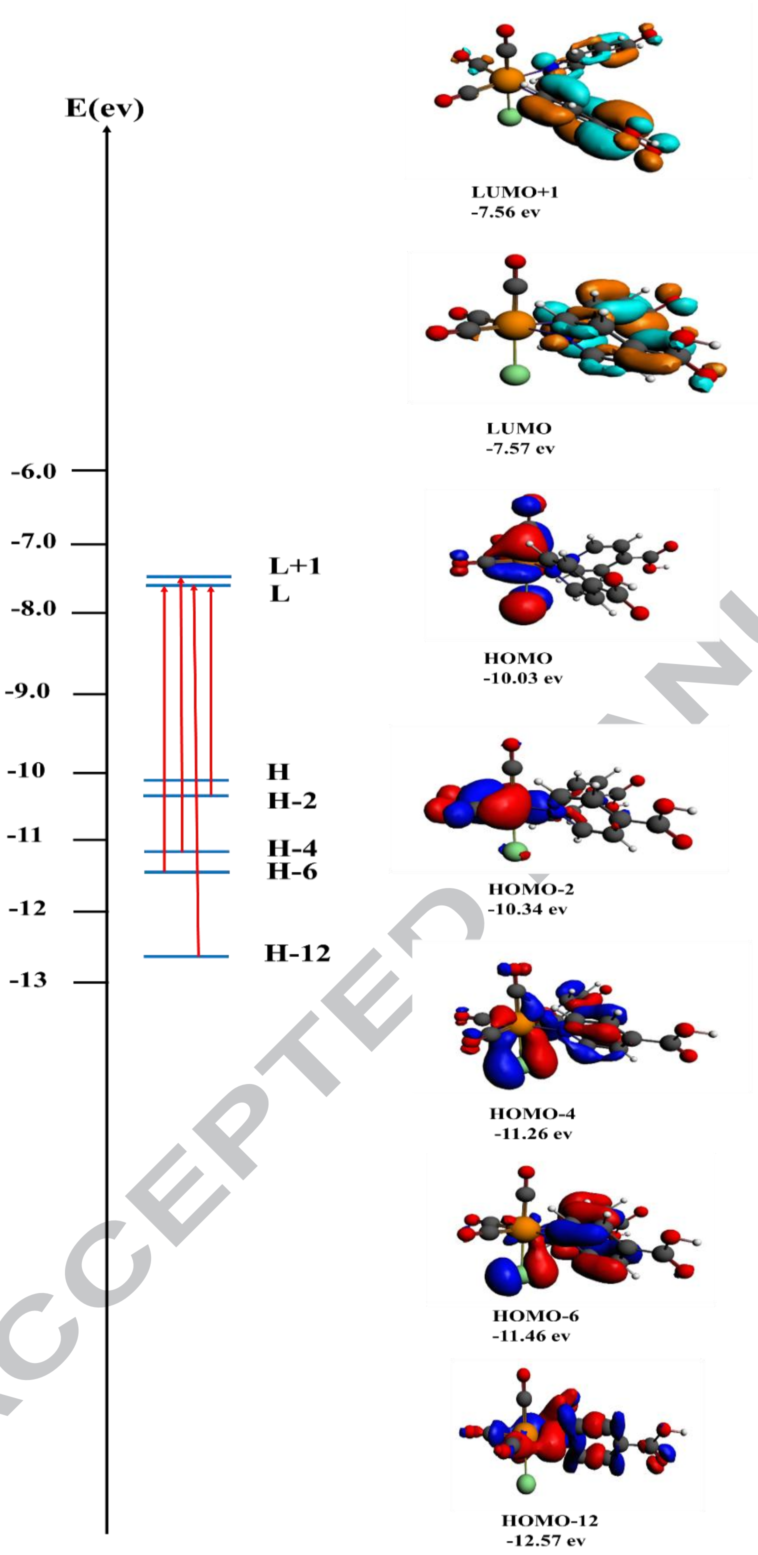

Figure 5. Qualitatively Molecular Orbital diagram for *fac*-Re(CO)$_3$(PyCOOH)$_2$Cl with the most important electronic transitions.

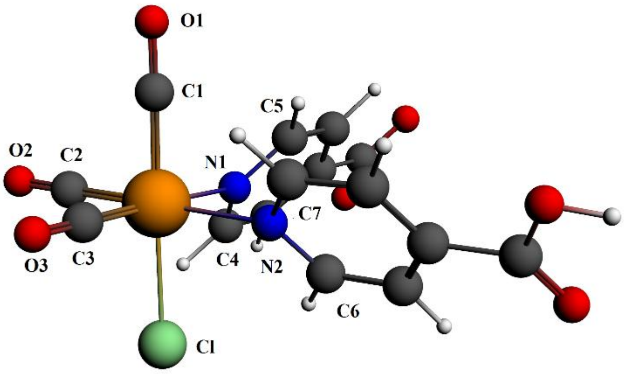

Figure 6. Scheme used in NBO analysis

Graphical abstract Pictogram

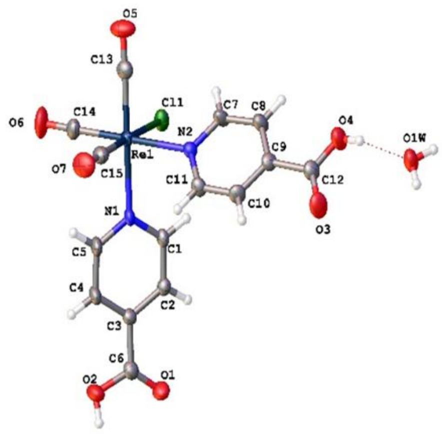

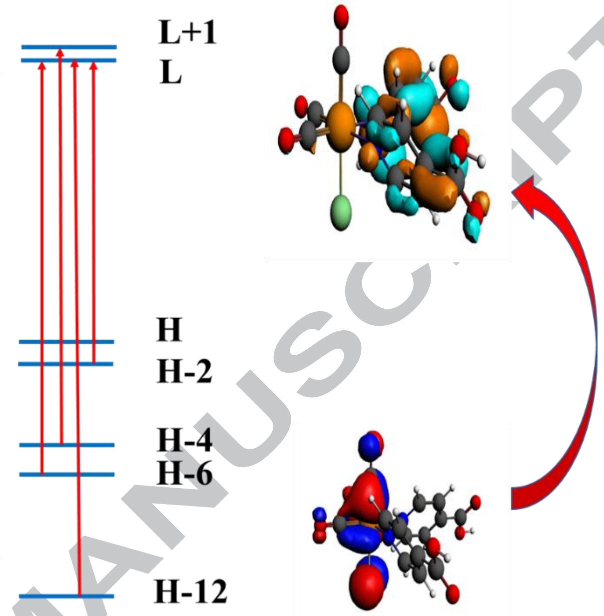

Highlights

- New d^6 transition-metal complex was prepared from isonicotinic acid ligand. This compound has been studied using relativistic two-component density functional theory.
- Relativistic DFT calculations suggest that experimental mixed absorption bands, which could be assigned to (MLCT-LLCT)/MLCT transitions
- The computational study of these compounds requires an accurate and efficient approach to treat the relativistic and solvent effects